Dynamic message-passing approach to epidemic spreading

Author: Adrià Meca Montserrat
Facultat de Física, Universitat de Barcelona, Diagonal 645, 08028 Barcelona, Spain.

Advisor: Matteo Palassini
(Dated: February 5, 2021)

Abstract: In this work, we delve into the analysis of the propagation of infectious diseases described by the SIR epidemiological model on networks whose connections change over time. We use a fast dynamic message-passing method to estimate the marginal probabilities that each node in one of these networks is in a given state at a certain time. After testing the validity of the predictions given by this approach, we apply them to the problem of inferring the origin of an epidemic on a dynamic network.

I. INTRODUCTION

The SARS-CoV-2 pandemic outbreak that has plunged the world into a severe sanitary crisis has highlighted the importance of studying the spread of infectious diseases through populations of individuals. However, this area of research has existed for many years. In fact, one of the earliest mathematical approaches to the spread of an epidemic is attributed to Daniel Bernoulli for his analysis of smallpox in 1766.

Today, epidemic spreading is studied using networks which are able to model the intricate contact patterns of human beings. An epidemiological model is also needed to identify the states of individuals with respect to some contagious disease. The unidirectionality of one of these models allowed the authors of [2] to present the *dynamic message-passing equations* as a closed set of recursion rules, which provide the probabilities that each member of a network is in a given state at time t.

In the present work, we have written from scratch an algorithm to test the validity of the dynamic message-passing (DMP) predictions on dynamic networks, by comparing them with the probabilities obtained using a *Monte Carlo simulation*. Then, we have adapted the code to be able to use the DMP probabilities to locate the origin of an epidemic from the observation of a given network at a certain time. We place great emphasis on the change of the links in a network, analyzing how it affects the DMP predictions and the performance of the aforementioned algorithm.

II. METHODS

A. SIR model

Epidemic modeling assumes that a population can be divided into different compartments depending on the stage of some contagious disease. In this work we adopt the SIR model in which individuals can be in one of the following three states at any given time: susceptible (S), infectious (I) or recovered (R). At each time step, an S individual can be infected by one of its I neighbors with probability λ, and an I individual can recover on its own with probability μ, regardless of its interactions. R individuals are removed from the contagion process, which makes the SIR model unidirectional [1–3, 7].

B. Networks

We model a population as a *network* (or *graph*) of N nodes. Each node i is connected to a set of neighbors $\partial i(t)$, whose size determines the degree c_i of the former. A node can have several properties, but we are mainly interested in its state $q_i(t)$ with respect to an infectious disease.

We use two types of networks: *random regular graphs* (RRG) which are selected uniformly at random from the set of graphs where all nodes have the same degree c [2, 4], and *proximity networks* (PN) which are created by placing N nodes uniformly at random in a square of side $\sqrt{N}$, and establishing links with probability

$$P_{ij} = \frac{c}{N} e^{-d_{ij}/l}, \tag{1}$$

where d_{ij} is the euclidean distance between nodes i and j, and l is a parameter that controls the presence of long connections [1].

We want to study the spread of epidemics on dynamic networks, so we need *rewiring algorithms* that can modify the connections of a given graph:

- For an RRG, we choose two links (i, j) and (k, m) at random, such that k and m are not connected to i or j, and with probability P_{rew} we remove the previous links and create the new connections (i, k) and (j, m). We refer to P_{rew} as *rewiring probability*;

- For a PN, we choose one link (i, j) and two nodes k and m at random, and with probability P_{rew} we remove the previous connection and create the new link (k, m).

Both algorithms are executed $Nc/4$ times, so there are $P_{\text{rew}}Nc/2$ link exchanges on average.

C. Dynamic message-passing equations

The epidemic process on a graph can be thought of as the spread of infection signals from I to S nodes [2], which enables us to introduce the messages:

$P_S^{k\to i}(t) \equiv$ probability that node k is susceptible at time t;

$\theta^{k\to i}(t) \equiv$ probability that an infection signal has not been passed from node k to node i up to time t;

$\phi^{k\to i}(t) \equiv$ probability that an infection signal has not been passed from node k to node i up to time t, and that node k is infectious at that moment.

The unidirectional nature of the SIR model allowed the authors of [2, 3] to present the dynamic message-passing equations as a closed set of recursion rules, which they wrote in terms of the above messages:

$$\begin{aligned} P_S^{k\to i}(t) &= P_S(0) \prod_{j\in\partial k(t)\setminus i} \theta^{j\to k}(t), \\ \theta^{k\to i}(t) &= \theta^{k\to i}(t-1) - \lambda\phi^{k\to i}(t-1), \\ \phi^{k\to i}(t) &= (1-\lambda)(1-\mu)\phi^{k\to i}(t-1) \\ &\quad - P_S^{k\to i}(t) + P_S^{k\to i}(t-1), \end{aligned} \tag{2}$$

where $P_S(0)$ is the probability that any node is initially susceptible, and $\partial k(t)\setminus i$ represents the set of neighbors of node k excluding node i. The DMP equations can be iterated over time, starting from the initial conditions $\theta^{k\to i}(0) = 1$ and $\phi^{k\to i}(0) = \delta_{q_k(0),\,I}$. They provide an estimate of the marginal probabilities that node i is in a given state at time t_0:

$$\begin{aligned} P_S^i(t_0) &= P_S(0) \prod_{k\in\partial i(t)} \theta^{k\to i}(t_0), \\ P_R^i(t_0) &= P_R^i(t_0-1) + \mu P_I^i(t_0-1), \\ P_I^i(t_0) &= 1 - P_S^i(t_0) - P_R^i(t_0). \end{aligned} \tag{3}$$

Even though the authors of [2, 3] used static graphs, here we generalize to dynamic networks for which we only need to know the neighbors of node i at time t, $\partial i(t)$, and the rewiring history. The computational complexity of the DMP equations is $O(tNc)$.

D. Validity of the DMP predictions

The marginal probabilities (Eqs. 3) given by the DMP equations (Eqs. 2) are exact for locally tree-like networks, to which RRGs tend to for large values of N. We use PNs as simple representatives of real-world networks. In this section, we check the validity of the DMP predictions on random dynamic networks by comparing them with the probabilities given by a Monte Carlo (MC) simulation.

Let us outline how the comparison is made: we create a dynamic network of N nodes, one of which is initially infectious and all the others are susceptible, and we let the system evolve up to time t_0. At that moment, we do an observation $\mathcal{O}$ of the entire network and the task is to calculate the probability that each of its nodes is in a given state X (i.e., S, I or R) using the MC simulation and the DMP equations, and compare the two. For a given initial graph and rewiring history,

- we perform a MC simulation that replicates the dynamic rules imposed by the SIR model up to time t_0. Repeating this M times we obtain the MC probability $P^i_{X,\mathrm{MC}}(t_0)$ that node i is in a given state X at time t_0. The uncertainty of $P^i_{X,\mathrm{MC}}(t_0)$ can be approximated by

$$\delta P^i_{X,\mathrm{MC}}(t_0) \simeq \sqrt{\frac{P^i_{X,\mathrm{MC}}(t_0)\big[1 - P^i_{X,\mathrm{MC}}(t_0)\big]}{M}}; \tag{4}$$

- we run the DMP equations on the graph up to time t_0. We only need to do this once to obtain the DMP probability $P^i_{X,\mathrm{DMP}}(t_0)$ that node i is in a given state at time t_0.

This entire process is a random instance of the problem of comparing the MC and DMP predictions. Running multiple instances gives us a collection of probabilities $P^i_{X,\mathrm{MC}}(t_0)$ and $P^i_{X,\mathrm{DMP}}(t_0)$ that we can sort by the values of the former in ascending order. This allows a clear comparison between the two methods.

E. Inference of the epidemic origin

The problem of inferring the origin of an epidemic is an example of one of the many applications of the DMP equations. It can be defined as follows: we generate a dynamic network of N nodes, one of which is initially infectious (the so-called patient zero, i_0) and all others are susceptible, and we let the system evolve until time t_0 is reached. At that moment, we do an observation $\mathcal{O}$ of the entire network and the task is to locate i_0.

Let us outline our approach to this problem: for each node i, whose state is either I or R in $\mathcal{O}$, we run the DMP equations on the initial graph up to time t_0. This gives us the probability $P_X^j(t_0, i)$ that node j is in a given state X at time t_0, assuming that node i is the patient zero. Bayes' theorem tells us that the probability that node i is the patient zero given the observation $P(i|\mathcal{O})$ is proportional to the probability of the observed states given the patient zero $P(\mathcal{O}|i)$. We approximate the latter as a product of the marginal probabilities provided by the DMP equations [2]

$$P(\mathcal{O}|i) \simeq \prod_{q_k(t_0)=S} P_S^k(t_0, i) \prod_{q_l(t_0)=S} P_I^l(t_0, i) \prod_{q_m(t_0)=S} P_R^m(t_0, i).$$

We also define an "energy" function $E(i) \equiv -\log P(\mathcal{O}|i)$, such that nodes with lower energy are more likely to be the true patient zero [2]. Once the iteration through the infectious and recovered nodes in $\mathcal{O}$ ends, we rank them by their energy value in ascending order, with zero being the lowest possible rank. Finally, we extract the rank of the true patient zero r_0. We refer to this whole process as random instance of the *inference algorithm*.

Instead of comparing the performance of the DMP-based inference algorithm with that of other inference measures [2], we analyze the effects of a higher rewiring probability on its efficiency.

III. RESULTS

A. Validity of the DMP equations

For a given time t_0, we compare the MC and DMP probabilities for 1000 instances on proximity networks of 1000 nodes and $l = 100$, and plot them as a function of their rank n. This can be repeated for higher values of P_{rew} to see if the agreement between the MC and DMP predictions changes significantly. As shown in Fig. 1, the probabilities of being infectious provided by the two methods are compatible, even when there is a non-zero value of P_{rew} acting on the graph. The rewiring disperses the DMP probabilities but has little impact on their mean values, which are close to the MC probabilities for all nodes.

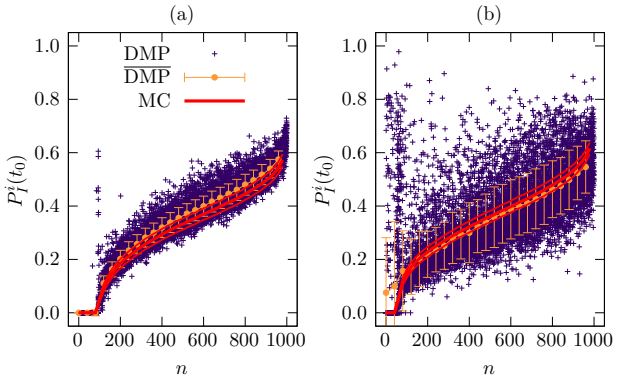

FIG. 1: Comparison of the MC and DMP probabilities for PNs of 1000 nodes and $l = 100$ (1000 instances). We generate an epidemic with $\mu = 0.5$, $\lambda = 0.7$ and $t_0 = 5$. The resulting probabilities are sorted by the values of $P^i_{I,\text{MC}}(t_0)$ and plotted as a function of their rank n. We denote the MC probabilities by a thick red line and their uncertainties by thin red lines calculated with the relation $P^i_{I,\text{MC}}(t_0) \pm \delta P^i_{I,\text{MC}}(t_0)$, where $\delta P^i_{I,\text{MC}}(t_0)$ is given by Eq. (4). We represent the values of the DMP probabilities by purple crosses and their average over the instances by orange dots, whose uncertainties are given by the standard deviation. (a) $P_{\text{rew}} = 0.0$; (b) $P_{\text{rew}} = 0.1$.

Another interesting study consists in observing if the MC and DMP predictions deviate significantly from each other for increasing values of t_0. Fig. 2 shows that the probabilities obtained by the two methods are compatible for all nodes at different observation times.

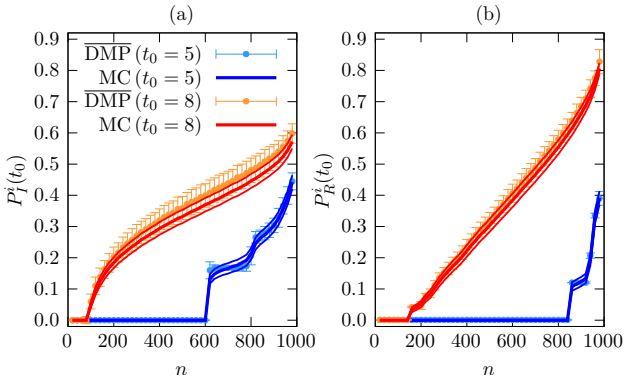

FIG. 2: Comparison between the MC and DMP probabilities for PNs of 1000 nodes and $l = 100$. We generate an epidemic with $\mu = 0.5$, $\lambda = 0.7$ and two values of t_0. The probabilities are sorted by the values of $P^i_{X,\text{MC}}(t_0)$ and plotted as a function of their rank n. We represent the MC probabilities by thick lines and their uncertainties by thin lines calculated with the relation $P^i_{X,\text{MC}}(t_0) \pm \delta P^i_{X,\text{MC}}(t_0)$, where $\delta P^i_{X,\text{MC}}(t_0)$ is given by Eq. (4). We represent the DMP probabilities averaged over 1000 instances by dots, whose uncertainties are given by the standard deviation.

To analyze the effect of the size of a network on the agreement between MC and DMP probabilities, we run ten instances on random regular graphs of 10^5 nodes and $c = 4$. As shown in Fig. 3, both methods provide very similar predictions despite using fewer instances. This can be attributed to the better performance of the DMP equations on large graphs, where the presence of short loops is scarce and nodes are more independent of each other. Furthermore, RRGs exhibit tree-like behavior as N increases, which accentuates the good results.

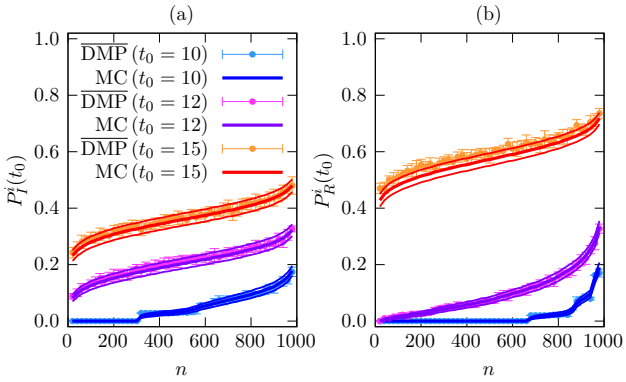

FIG. 3: Comparison of the MC and DMP probabilities for 10 instances on RRGs of 10^5 nodes and $c = 4$. An epidemic is generated with $\mu = 0.5$, $\lambda = 0.7$ and several values of t_0. We generate this figure in the same way as Fig. 2.

B. Inference of the epidemic origin

Now, we present the results of the problem of inferring the origin of an epidemic, starting with two instances of the inference algorithm with different values of P_{rew} on RRGs of 1000 nodes and $c = 4$. We plot the resulting energies of the nodes as a function of their rank; see inset of Fig. 4. Since single instances are not enough to draw conclusions, we set the value of P_{rew} and run a thousand instances of the inference algorithm, each of which gives a normalized rank of the true patient zero $r_0/|G|$ (i.e., r_0 divided by the number of infectious and recovered nodes in the observation $\mathcal{O}$). A histogram is used to show the results of this process for several values of P_{rew}; see Fig. 4. The inference algorithm is able to predict the location of the true patient zero with greater precision than 60% for values of P_{rew} up to 0.3. We must bear in mind that with this configuration there is an average of 600 link exchanges at each time step (i.e., approximately a third of all the links present in a RRG of 1000 nodes and $c = 4$), which makes the results surprising. Increasing values of P_{rew} have less impact on the performance of the inference algorithm. In fact, the histogram seems to indicate that there is a saturation of the efficiency of the algorithm for higher values of the rewiring probability. That, however, should be investigated in more detail in future work.

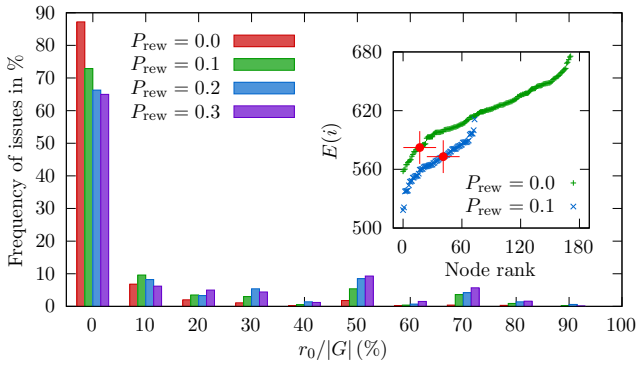

FIG. 4: Results of 1000 instances of the inference algorithm on RRGs of 1000 nodes and $c = 4$. Inset: an epidemic is generated with $\mu = 1$, $\lambda = 0.6$ and $t_0 = 8$. The energies of the nodes provided by the inference algorithm are plotted as a function of their rank for two random instances with different values of P_{rew}. The true patient zero is marked by a red cross in both cases. Main figure: an epidemic is generated with $\mu = 1$, $\lambda = 0.5$ and $t_0 = 5$. The histogram (over 1000 instances) of the normalized rank of the true patient zero $r_0/|G|$ (where $|G|$ is the number of I and R nodes in $\mathcal{O}$) is plotted for several values of P_{rew}.

Next we let one of the parameters (i.e., μ, λ or t_0) vary to study how it affects the efficiency of the algorithm. Let us start with λ: for each of its values, we average $r_0/|G|$ over 1000 instances. At the end of this procedure, we possess a set of ordered pairs $\{(\lambda, \langle r_0/|G|\rangle)\}$ that we can plot. Repeating this whole process for different values of P_{rew} it is possible to analyze its effect on the performance of the inference algorithm. As expected, Fig. 5a shows that increasing values of P_{rew} complicate the task of inferring the epidemic origin. However, the predictions are still good. The same study can be done for t_0; see Fig. 5b. Here we observe that the inference algorithm is able to predict successfully the patient zero before the epidemic peak occurs. For later observation times the predictions are worse, but by then the study of the patient zero loses interest since it cannot be applied to contain an epidemic outbreak.

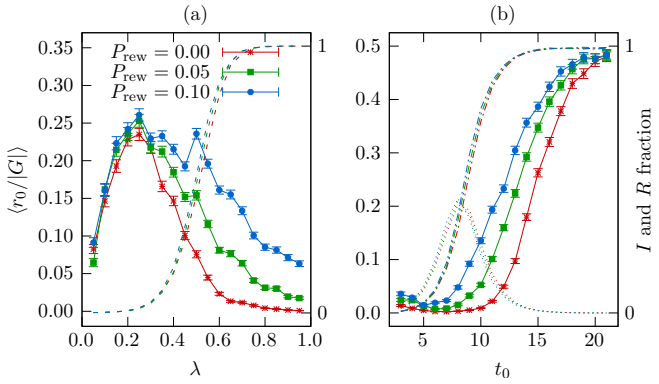

FIG. 5: Normalized rank of the true epidemic origin averaged over 1000 instances of the inference algorithm on RRGs of 1000 nodes and $c = 4$. (a) We set $\mu = 0.5$ and $t_0 = 10$, and let λ vary to study how $\langle r_0/|G|\rangle$ depends on it. We repeat this process for several values of P_{rew} to see if they affect the efficiency of the inference algorithm. The dashed lines show the average fraction of nodes that are infectious or recovered in $\mathcal{O}$ for each value of P_{rew}. (b) We set $\mu = 0.5$ and $\lambda = 0.7$, and let t_0 vary to study how $\langle r_0/|G|\rangle$ depends on it. This process is repeated for multiple values of P_{rew} to see if they affect the performance of the inference algorithm. The dotted and dash-dotted lines show the average fraction of I and R nodes in $\mathcal{O}$ for each value of P_{rew}, respectively.

Finally, to see how the intrinsic parameters of a graph can alter the results of the inference algorithm, the above analysis for λ can be performed on proximity networks of 1000 nodes with different values of l. Fig. 6 shows that this parameter can change the performance of the algorithm significantly. One the one hand, for $l = 10$ (Fig. 6a) we favor the presence of local connections in the networks, and the predictions get worse. Curiously, they improve for higher values of both P_{rew} and λ, which can be attributed to the addition of long connections by the rewiring algorithm. On the other hand, for $l = 100$ (Fig. 6b) proximity networks behave like Erdős-Rényi graphs (ER), i.e., random networks of N nodes in which each one of the $N(N-1)/2$ possible connections is present with probability P [7]. In turn, ERs tend to RRGs for large N and constant P, which explains why Figs. 5a and 6b are so alike. Although in the latter the effect of the rewiring algorithm is less noticeable, which again could be explained by the addition of longer interactions. In

fact, if we take a closer look at Fig. 6 we can see that the rewiring algorithm makes the fraction of I and R nodes in the observation grow significantly, which indicates the sparsity of long links when P_{rew} is zero.

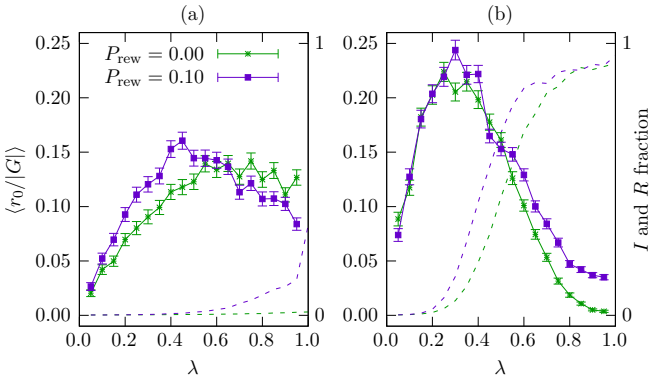

FIG. 6: Normalized rank of the true epidemic origin averaged over 1000 instances of the inference algorithm on PNs of 1000 nodes with different values of l. We set $\mu = 0.5$ and $t_0 = 10$, and let λ vary to study how $\langle r_0/|G|\rangle$ depends on it. We repeat this process for several values of P_{rew} to see if they affect the efficiency of the inference algorithm. The dashed lines show the average fraction of nodes that are infectious or recovered in $\mathcal{O}$ for each value of P_{rew}. (a) $l = 10$; (b) $l = 100$.

IV. DISCUSSION

In this work, we have verified the validity of the DMP equations on dynamic networks, which has been done through a comparison between the DMP predictions and the probabilities provided by a MC simulation. In fact, since the results given by both methods are so similar we should use the more efficient of the two. In that regard, the DMP approach is superior to the MC simulation, as the former only needs one run on a given graph to provide the marginal probabilities of interest, and the latter requires multiple executions.

Then we have applied the DMP approach to study the problem of determining the origin of an epidemic. This problem had already been studied by the authors of [2] to showcase the potential of the DMP method when applied to static networks. We have generalized their approach to dynamic networks and have shown that the DMP-based inference algorithm continues to perform well on them.

The DMP equations had been studied before in the literature [1–3, 5], but its interest has recently resurfaced due to the SARS-CoV-2 pandemic. In that regard, the DMP method could be applied to obtain the marginal probability that each person in a large city is infectious at a given time. Then we could test the individuals with a higher probability of being infected according to the DMP method, and confine them if necessary [1]. Even though we already have the necessary tools to implement an algorith like this, it could not describe a disease as complicated as SARS-CoV-2. For that, we would have to use more complex networks, like those utilized in [1], and adopt an epidemiological model with more than three possible states. We leave this task for future work.

V. CONCLUSIONS

We can conclude that our results corroborate the agreement between the MC and DMP predictions on random dynamic networks, the latter approach being more efficient since it only requires one run per network. Therefore, it is justified to use an inference algorith based on the DMP equations to study the problem of inferring the origin of an epidemic on dynamic networks. Here the rewiring worsens the efficiency of the inference algorithm, but it can still give good results.

Acknowledgments

I would like to thank my mother for her support, and my advisor Matteo Palassini for his patience and help in the development of this work.

[1] Antoine Baker, Indaco Biazzo, Alfredo Braunstein, et al., *Epidemic mitigation by statistical inference from contact tracing data*, arXiv:2009.09422 (2020).

[2] Andrey Y. Lokhov, Marc Mézard, Hiroki Ohta, et al., *Inferring the origin of an epidemic with a dynamic message-passing algorithm*, Phys. Rev. E **90**, 012801 (2014).

[3] Andrey Y. Lokhov, Marc Mézard, Lenka Zdeborová, *Dynamic message-passing equations for models with unidirectional dynamics*, Phys. Rev. E **91**, 012811 (2015).

[4] A. Steger and N. Wormald, *Generating random regular graphs quickly*, Probability and Computing 8 (1999), 377-396, 1999.

[5] Brian Karrer and M. E. J. Newman, *A message-passing approach for general epidemic models*, arXiv:1003.5673 (2010).

[6] M. Newman, *Networks* (second edition), Oxford University Press, United Kingdom (2018).

[7] Romualdo Pastor-Satorras, Claudio Castellano, Piet Van Mieghem, Alessandro Vespignani, *Epidemic processes in complex networks*, Rev. Mod. Phys. **87**, 925 (2015).